nature climate change

Article

https://doi.org/10.1038/s41558-025-02325-x

High-income groups disproportionately contribute to climate extremes worldwide

Received: 8 November 2024

Accepted: 24 March 2025

Published online: 7 May 2025

Check for updates

Sarah Schöngart[1,2,3] ✉, Zebedee Nicholls[1,4,5], Roman Hoffmann[1], Setu Pelz[1] & Carl-Friedrich Schleussner[1,3]

Climate injustice persists as those least responsible often bear the greatest impacts, both between and within countries. Here we show how GHG emissions from consumption and investments attributable to the wealthiest population groups have disproportionately influenced present-day climate change. We link emissions inequality over the period 1990–2020 to regional climate extremes using an emulator-based framework. We find that two-thirds (one-fifth) of warming is attributable to the wealthiest 10% (1%), meaning that individual contributions are 6.5 (20) times the average per capita contribution. For extreme events, the top 10% (1%) contributed 7 (26) times the average to increases in monthly 1-in-100-year heat extremes globally and 6 (17) times more to Amazon droughts. Emissions from the wealthiest 10% in the United States and China led to a two- to threefold increase in heat extremes across vulnerable regions. Quantifying the link between wealth disparities and climate impacts can assist in the discourse on climate equity and justice.

Over the past two decades, extreme events attributable to climate change resulted in an annual average of US$143 billion in damages[1]. How these costs could and should be covered—both between and within countries—is a matter of debate[2]. Central to this debate is the stark disparity between those responsible for emissions and those affected by their impacts. The wealthiest 10% of the global population accounted for nearly half of global emissions in 2019 through private consumption and investments, whereas the poorest 50% accounted for only one-tenth of global emissions[3]. At the same time, regions with low historic emissions and income levels are typically more frequently and severely exposed to climate impacts[4,5] and have limited resources for adaptation[6]. This cause-and-effect injustice is widely acknowledged[7], yet a quantification of how emissions inequality translates into unequal accountability for the resulting global temperature levels and extreme climate events is missing. This translation should account for the individual warming contributions of emissions of non-CO_2 GHGs, such as methane (CH_4), given their major role in recent warming[8].

In this study we combine wealth-based carbon inequality assessments[3] with an emulator-based climate modelling framework[9] to systematically attribute changes in global mean temperature (GMT) levels and grid-cell-level climate extremes to emissions from different wealth groups. We use the Model for the Assessment of the Greenhouse Gas Induced Climate Change (MAGICC)[10], a simple climate model, in conjunction with the Modular Earth System Model Emulator for Monthly Temperature and Precipitation (MESMER-M-TP)[11], a model that is able to generate large ensembles of spatially explicit monthly temperature and precipitation data that closely resemble those of complex Earth system models at a fraction of the cost.

We use attribution science frameworks to link human-induced GHG emissions to changes in the modelled frequency and intensity of extremes[12]. These frameworks were originally developed to attribute changes in total human emissions[13,14]. Today, they are increasingly applied for source attribution; that is, to quantify the relative contributions of individual emitter groups, such as companies or countries[15,16]. When attributing impacts among multiple emitters, various approaches exist and serve distinct purposes[17,18]. Here we assess the changes in the characteristics of monthly extremes but for the emissions attributable to a specific emitter group[15,18].

[1]International Institute for Applied Systems Analysis (IIASA), Laxenburg, Austria. [2]Institute for Atmospheric and Climate Science, ETH Zürich, Zurich, Switzerland. [3]IRIThesys, Humboldt-Universität zu Berlin, Berlin, Germany. [4]Climate Resource, Melbourne, Victoria, Australia. [5]School of Geography, Earth and Atmospheric Sciences, The University of Melbourne, Melbourne, Victoria, Australia. ✉e-mail: sarah.schoengart@env.ethz.ch

https://doi.org/10.1038/s41558-025-02325-x

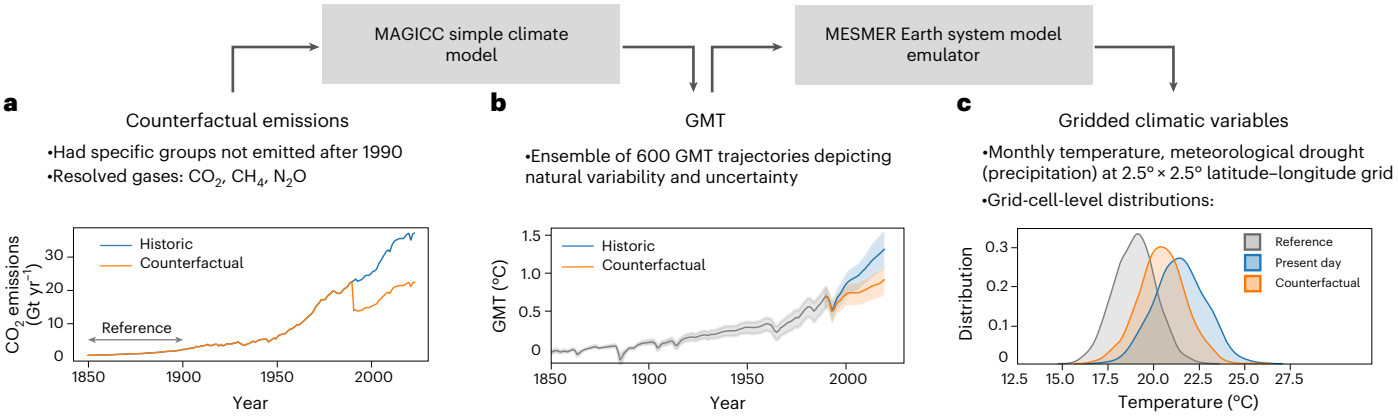

Fig. 1 | Overview of the modelling framework using a schematic example. Counterfactual emissions were converted into GMT using the simple climate model MAGICC and subsequently translated into grid-cell-level realizations of climatic variables using MESMER-M-TP. **a**, Counterfactual CO_2 emissions pathways. Historic emissions with and without contributions from selected emitter groups after 1990 (orange). **b**, Median GMT levels for historic and counterfactual emissions pathways (solid lines) along with 5th–95th confidence intervals (shaded envelopes) derived from 600 ensemble members. **c**, Reference, present-day and counterfactual distributions at a single grid-cell using temperature as an example.

We generate counterfactual emission pathways by subtracting the 1990–2019 emissions of specific emitter groups, namely the wealthiest 10%, 1% and 0.1% globally, as well as in the United States, EU27, India and China (Fig. 1b). Emissions data are drawn from ref. 3 and include emissions from domestic consumption, public and private investments and trade. These emissions are attributed primarily to consumers, except emissions from capital formation in production sectors, which are attributed to firm owners[3]. Emissions are reported as a basket of GHGs with warming expressed in CO_2 equivalents. We convert these counterfactual pathways into GMT levels and gridded climatic variables (Fig. 1a), allowing us to compare the 2020 climate against the hypothetical 2020 climate state that we would observe if these groups had not emitted. Specifically, we attribute GMT levels and changes in the probability and intensity of extremely hot and dry months (Fig. 1c). Prolonged heat poses a significant burden on human health[19] and sustained precipitation deficits impair crop yields and threaten water resources[20], meaning that both climate extremes are highly relevant in driving climate impacts. We measure meteorological droughts with the standardized precipitation index computed over 3-month periods (SPI-3)[20].

We quantify climate impacts associated with wealthy emitters and compare them to the global average per capita contribution. We do not assess what would constitute fair or just emissions, nor do we assign direct responsibility for the resulting impacts. For illustration, we also provide counterfactual warming outcomes based on rescaling global emissions according to the per capita profile of individual income percentiles.

Inequality in attributed global warming contributions

Our modelling framework depicts natural variability and uncertainty in the global response to emission changes (Methods). Unless mentioned otherwise, we provide median results with the 5th–95th confidence intervals in parentheses. All results are statistically significant (established via a one-sample *t*-tests, Methods) unless explicitly marked otherwise. As our database provides only basket emissions, we derived the main results by assuming that emissions for each GHG scale proportionally with the globally aggregated emissions (Methods). We explore the sensitivity to this assumption in Supplementary Section 2.

GMT in 2020 is 0.61 °C (0.45–0.83 °C) higher than in 1990. We found that about 65% (0.40 °C (0.27–0.56 °C)) of this increase is attributable to the global top 10%, 20% (0.12 °C (0.09–0.17 °C)) to the top 1% and 8% (0.05 °C (0.03–0.07 °C)) to the top 0.1% (Fig. 2a and Supplementary Table 3). These warming contributions are higher (by about one-fifth) than the respective group's contributions to aggregated GHG basket emissions (Supplementary Table 2), underscoring the importance of non-CO_2 GHGs[21] (see also Supplementary Section 2).

To put these numbers into perspective, we defined a group's equal share as the contribution to warming they would have if their per capita impact matched the global average. Therefore, we scaled the total GMT increase according to the group's share of the global population (for example, the equal share of the global top 10% would be 10% of the full 0.61 °C increase). We then derived climate inequality factors (CIFs) as the group's actual contribution to global warming relative to their equal share. CIFs increase from 6.5 for the top 10% to 20 (77) for the top 1% (0.1%), indicating an amplification of climate inequality with increasing wealth.

The full depth of the disproportion in contributions to GMT level becomes tangible when global emissions are rescaled according to the per capita profile of global income groups (Fig. 2b). If the entire world population had emitted like the bottom 50%, there would have been minimal additional warming since 1990. However, if the entire world population had emitted like the top 10%, 1% or 0.1%, the GMT increase since 1990 would have been 2.9 °C, 6.7 °C or 12.2 °C.

Between 1990 and 2020, emissions from the global top 10% arose primarily in the world's highest emitting countries: the United States, the EU27, China and India (Fig. 2c). Note that the composition of the global top 10% shifts over time (Supplementary Fig. 1), and while our focus is on wealthy individuals from the world's largest economies, those from smaller (wealthier, as well as less wealthy) countries also contribute disproportionately[3]. Income levels from regional top emitters deviate from their global counterparts: the top 10% and 1% in the United States and the EU27 (India and China) are wealthier (poorer) than the globally wealthiest 10% and 1% (Fig. 2d).

Attributed GMT shares by regional emitter groups combine within- and between-region inequality. In the United States (EU27), the top 10% contribute 3.1 (2.8) times more to global warming than the average citizen, but 17 (8) times more than the global average. For the United States, the contribution of the top 10% alone exceedes the entire country's equal share. This relative inequality increases with increasing wealth: the top 1% in the United States (EU27) contribute 53 (21) times their equal shares, and the top 0.1% contribute 190 (64) times their equal shares. In China, where the overall CIF is near 1, the top 10%, 1% and 0.1% emit 4, 13 and 50 times their equal shares, showing even greater regional influence from societal elites. Similarly, in India, where the national CIF is 0.3 (implying that the countries per capita average emissions are below the global average), the top 10%, 1% and 0.1% emit 1.2, 4 and 10 times the global average.

https://doi.org/10.1038/s41558-025-02325-x

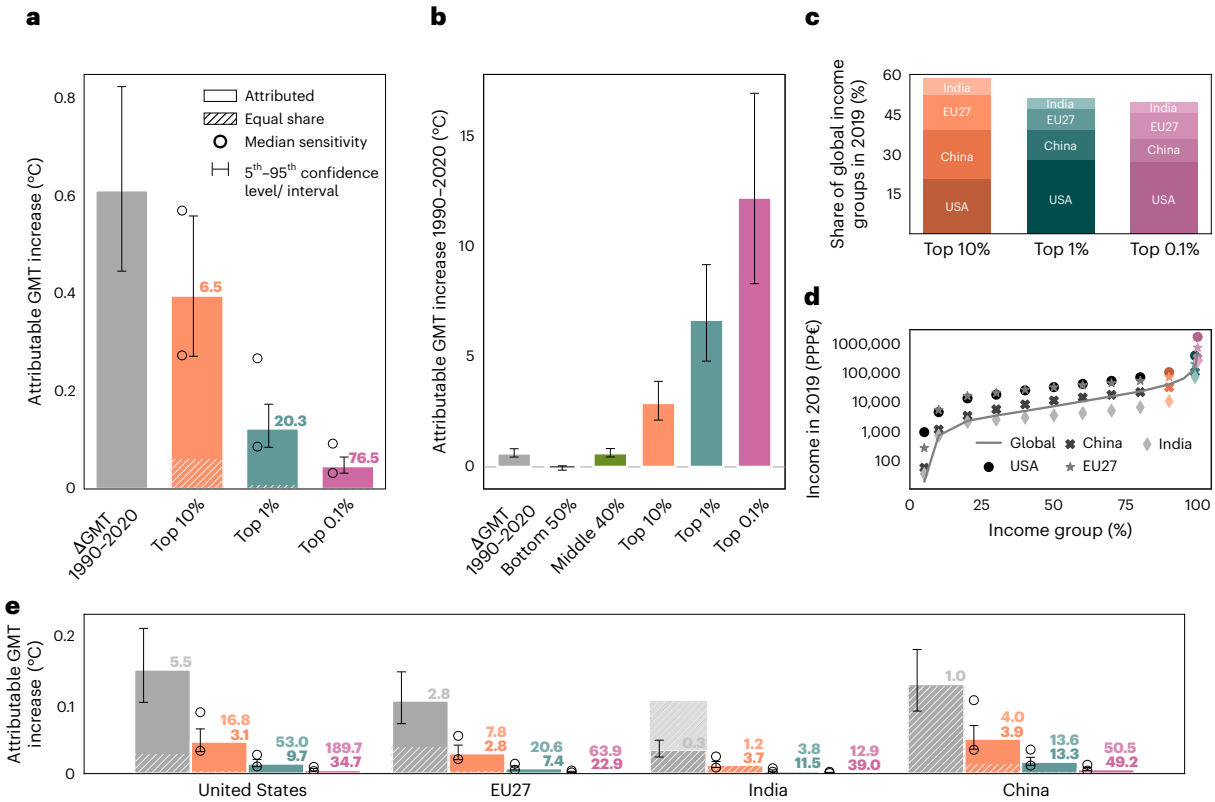

Fig. 2 | Attributed 1990–2020 GMT increases by emitter group. a, Median GMT increase over 1990–2020 and the shares attributed to global top 10%, 1% and 0.1%. Hatched areas indicate the warming for each group based on an equal per capita contribution to warming. CIFs indicating the group's contribution to global warming relative to the average contribution are given above the bars. Vertical lines represent the 5th–95th confidence intervals from natural variability and uncertainty in the global temperature response. Circles highlight median values from the sensitivity analysis (Methods; the lower circle is CO_2-based emissions and the upper circle is non-CO_2-based emissions). Estimates are based on 600 ensemble members each. **b**, Median hypothetical GMT increase from 1990–2020 if everyone emitted like the given income groups, with the 5th–95th confidence intervals represented as vertical lines. Estimates are based on 600 ensemble members. **c**, Regional breakdown of the global top 10%,1% and 0.1% in 2019. **d**, Global (solid line) and regional (symbols) income distributions in 2019. **e**, Same as **a** but for the regional top 10%, 1% and 0.1% in the United States, the EU27, India and China. Grey bars highlight the median GMT increase attributable to each region as a whole. Two CIFs are given: the lighter (darker) value is relative to the country's equal share (actual emissions) and measures global (regional) inequality. Vertical lines represent the 5th–95th confidence intervals from natural variability and uncertainty in the global temperature response. Circles highlight median values from the sensitivity analysis. Estimates are based on 600 ensemble members each.

Major disparities in attributable extremes worldwide

We attribute regional increases in the frequency of extremely hot (dry) months, here defined as 1-in-100-year events in a pre-industrial climate, to the emissions of the global top 10% (Fig. 3a), so throughout this Article extremes or extreme events refer to a month being at least as hot (dry) as the hottest (driest) 1% of months in a pre-industrial climate. We state attribution results as additional event counts over a modelled 100-year period of current climate conditions compared with those in 1990 (Methods). For example, 10 additional attributable events indicate that a pre-industrial 1-in-100-year event happens an additional 10 times within 100 years, meaning that its probability has increased tenfold.

For heat extremes, changes are most (least) pronounced in August (February), where 11.5 [8.5–15.4] (3.5 [2.4–4.3]) additional events are attributable to the global top 10%. These changes refer to the global median over land that is predominantly located on the Northern Hemisphere. Areas in strongly affected regions, such as the Amazon region, Southeast Asia or central Africa, face months with up to 30-fold increases in probability (see also Supplementary Figs. 5–8).

To account for differences in seasonality between the Northern Hemisphere and Southern Hemisphere, we assessed heat extremes during the month with peak temperatures (Supplementary Fig. 4). Emissions from 1990–2020 led to a 12.3-fold (9.7–17.9) increase in the probability of heat extremes in the peak temperature month. The top 10% (1%) contribute 7.3 (25.7) times the global average to this (Supplementary Figs. 9–13e). In addition, the intensities of these extremes increased by 0.83 °C (0.75–0.97 °C) since 1990. Of this increase, 0.55 °C (0.50–0.67 °C) (0.17 °C (0.16–0.21 °C)) is attributable to the top 10% (1%), suggesting that their contribution is 6.7 (21.1) times higher than the global average (Supplementary Figs. 9–13).

Attribution results for meteorological drought extremes strongly depend on region and month, with robust drying found mainly in Central America, the Amazon, the Mediterranean, southern Africa and northern Australia (Fig. 3d and Supplementary Figs. 5–8). This is expected, given the considerable intermodel disagreement and large uncertainties in regional precipitation projections[22–24]. We found the strongest attributable drying trend in the Amazon region in October. Overall, the region faces a threefold increase (1.7–4.2) in extreme probability compared with 1990 (Fig. 3b). The top 10% (1%) contribute 6.1 (16.7) times the global average to this increase. The Amazon region is of global importance, given its uniquely biodiverse system and its major role in the global carbon cycle. Drought events over the past century have already negatively impacted carbon storage in Amazonian rainforests[25].

Overall, the spatial disparity in attributable changes at the grid-cell-level (Fig. 3 and Supplementary Figs. 5–13) implies that the regions that disproportionately contribute to the emissions of the top 10% (for example, the EU27 and the United States; Fig. 2) face smaller increases than regions that have contributed very little (for example,

https://doi.org/10.1038/s41558-025-02325-x

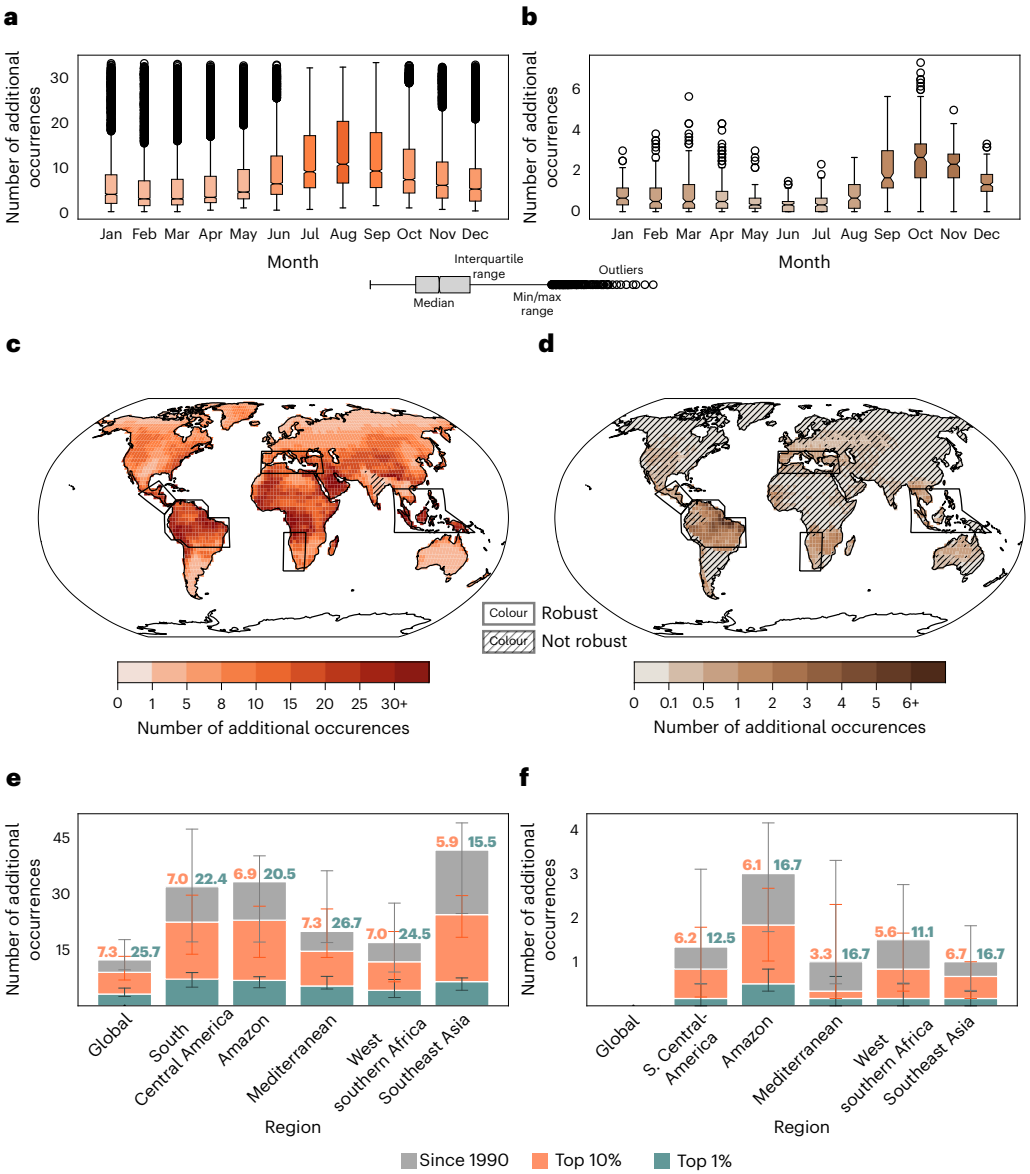

Fig. 3 | Frequency change of 1-in-100-year monthly heat and meteorological drought events attributable to global top emitters. a,**b**, Monthly distributions of heat extremes (**a**) and drought extremes in the Amazon (**b**) across grid cells attributable to the global top 10%. Distributions were derived by first computing the median attribution results at each grid cell (estimated from 15,000 ensemble members each) and then computing statistics across all 2,652 grid cells. Colour shading is qualitative. **c**,**d**, Spatial distribution of the median number of heat (**c**) and drought (**d**) extremes during peak temperature months attributable to the global top 10%. Median estimates are derived from 15,000 ensemble members. Hatched regions indicate insignificant results and/or insufficient model agreement. **e**,**f**, Median number of additional heat (**e**) and drought (**f**) extremes by region (highlighted on the maps in **c** and **d**). CIFs indicating the group's contribution to extremes relative to the average contribution are given above the bars. Vertical lines correspond to 5th–95th confidence intervals. We omit showing global drought estimates because of insufficient agreement among grid-cells. Distributions were derived by first computing median attribution results at each grid cell (estimated from 15,000 ensemble members each) and then computing statistics across all grid cells within each region.

western North America and west and central Europe compared with the Amazon region and west southern Africa in Fig. 3c,d).

The relatively small (attributable) changes over India and parts of China and the simultaneously high intermodel disagreement are worth noting, given that they are inconsistent with the increasing number of climate-related disasters India is already facing[26]. We assume that this is related to the climate effects of air pollution, which we discuss in greater detail in Supplementary Section 3.

Attributing transboundary impacts of regional emissions

The inequality in warming contributions from affluent groups in high-emitting regions exceeds the inequality in their global counterparts (Fig. 2). This disparity also appears at the grid-cell-level: in the global median, emissions from the top 10% (1%) in the United States are associated with 1.3 (1.0–1.8) (0.3 (0.3–0.5)) additional 1-in-100-year heat events during peak temperature months. This impact represents 23 (60) times the global average contribution and about 3 (2) times the relative contribution of the global top 10% (1%) (Fig. 3). The increase in extreme heat is unevenly distributed across regions. For example, in heat-affected areas such as the Amazon and southeast Africa, emissions from the top 10% in China (the United States) are linked to 2.7 (1.9–3.2) (2.5 (1.7–2.8)) and 2.7 (1.1–3.4) (2.5 (1.0–3.2)) additional occurrences of extreme heat during months with peak temperatures (Fig. 4). In these areas, we can also robustly attribute heat extremes to the regional top 1%. In the Amazon, 0.8 (0.7–1.0) additional heat extremes are

https://doi.org/10.1038/s41558-025-02325-x

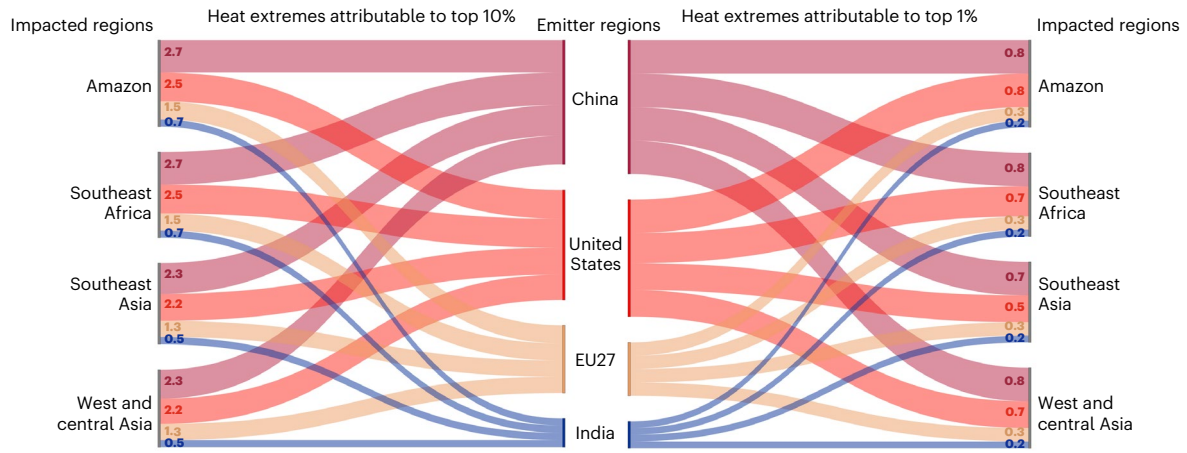

Fig. 4 | Increase in the frequency of 1-in-100-year peak summer heat extremes in selected regions attributable to the top 10% and 1% of emitters. Left: median number of additional heat extremes in selected regions that are attributable to the top 10% of emitters in China, the United States, the EU27 and India. Right: same as on the left but for the top 1% of emitters. Wider bars indicate that more events are attributable to a given emitter group. The values in the bars indicate the additional numbers of events over the course of 100 years. Median estimates were derived by first computing median attribution results at each grid cell (estimated from 15,000 ensemble members for each) and then computing statistics across grid cells within each region.

attributable to the top 1% in China. This corresponds to an increase in occurrence frequency of 80%.

Attributing changes in extreme events to country-specific wealthy emitter groups becomes increasingly challenging as emitter groups decrease in per capita size, meaning that their cumulative emissions decrease even if their relative emissions contributions increase. Projected temperature distributions are characterized by strong changes in the trend and by consistency across models, allowing robust attribution results even for seemingly small emission amounts, particularly in highly affected regions. The magnitude depends on the definition of extremes, with tail risks seeing the strongest increase (Supplementary Figs. 18–21). For droughts, the situation is more complex. The SPI-3 signal is dominated by variability and considerable intermodel disagreement, which prevented us from deriving robust attribution results when emissions are small.

Discussion

This study introduces a framework to link wealth-based emissions to shifts in GMT and to changes in regional monthly heat and meteorological drought extremes. We found that the wealthiest 10% contributed 6.5 times more to global warming than the average, with the top 1% and 0.1% contributing 20 and 76 times more, respectively. For heat, this imbalance is more pronounced at the grid-cell-level: the wealthiest 10% and 1% contributed over 7 and 25 times more than the global average to the increase in frequency of pre-industrial 1-in-100-year heat extremes during months with peak summer temperatures. The warming contributions of the wealthy are associated with considerable transboundary effects—for example, the contributions of the wealthiest 10% within the United States and China led to a two- to threefold increase in heat extremes across vulnerable regions such as the Amazon, Southeast Asia and southeast Africa. The robust attribution of drought signals is more complex. We found the strongest signals in the Amazon region in October, where the emissions of the global top 10% (1%) led to a 2.3-fold (0.8-fold) increase in the frequency of extreme droughts.

Our analysis also underscores the critical role of CH_4 emissions in near-term warming (Supplementary Fig. 2) and calls for new research to disentangle income-based emissions at the level of individual gases. Reducing CH_4 emissions in line with Paris Agreement-compatible pathways could yield immediate reductions in global temperatures and climate extremes[27].

We note that our study focuses on monthly extreme heat (that is, extremely hot months), meaning that heatwaves—defined as prolonged periods of abnormally high temperatures lasting from two days to months[28]—do not directly relate to our metric. However, the probability of extreme daily temperatures is amplified during extremely hot months[29], implying that attributable results for short-duration heatwaves might be even more pronounced. Further research is needed to explicitly explore this relationship.

Wealth-based emissions comprise private consumption and investment in capital formation across production sectors that supply goods and services consumed by society. Recognizing the associated unequal warming contributions can inform policy interventions. For example, deliberation over a coordinated global wealth tax can draw on this work, illustrating the climate co-benefits of attenuating stark wealth-based disparities in climate impact responsibilities[30,31]. The transboundary impacts we identify highlight how high-emitting individuals contribute to intensified extremes, even in distant regions. Similarly, the warming attributable to the investments of the wealthy underscores the need to realign financial flows to meet global climate goals[32]. This is particularly relevant for the wealthiest 1% and 0.1%, whose transboundary contributions to worsening local extremes arise primarily through investments, rather than consumption. Efforts to redirect these financial flows should also consider the shared responsibilities of governments to expedite systemic changes in financial and regulatory structures[33].

Our granular impact analysis shows that low-income regions incur the brunt of the harm caused by emissions concentrated among wealthier populations worldwide. From an adaptation and loss-and-damage perspective, this provides a basis for policy discussions around contributions to compensatory and preventative measures. The amounts of adaptation and loss-and-damage finance provided currently are minuscule compared with the assessed needs[34]. Our work motivates innovative policy instruments targeted at wealthy individuals to bridge these glaring finance gaps[35]. Such policies can also improve perceptions of climate justice, a vital factor in fostering social acceptance of climate action[36,37]. Moving towards evidence-based and targeted policies that reflect polluter-pays principles, including on the domestic level in terms of individual contributions, may therefore be an important cornerstone to enhance policy support for climate action in general.

Considerations of our results in policy debates must, however, recognize the conceptual challenges and value judgements in our approach and implementation. First, our attribution relies on consumption-based emissions accounting, allocating emissions between consumers and shareholders through shared ownership (see ref. 3). Our approach contrasts with production-based approaches used to quantify the responsibilities of producers[15]. Exploring diverse accounting frameworks is key to developing policy mechanisms that address multiple dimensions, but requires care in determining responsibility. Second, we employ the 'but for' attribution method. This approach directly links emissions to observed climate change while accounting for the timing of emissions and impacts. However, it is sensitive to the sequence of emissions removal and the design of the counterfactual scenarios[18]. Third, our approach is limited to changes in climate hazards only, and does not account for on-the-ground vulnerabilities and exposure, which are often key to driving the eventual impact of extreme climate events[38]. Integrating other causal drivers into extreme event attribution analysis increasingly allows us to address those limitations[38,39] in a step towards using extreme event attribution to inform the discourse on loss and damage[40,41]. At the same time, wealth levels are a key determinant for adaptive capacity and vulnerability in the face of climate change, particularly at the levels of households and individuals[42,43]. We would therefore expect wealth-related drivers of vulnerability and exposure to further exacerbate the inequalities in responsibilities and experience of the impacts of the climate hazards we studied here.

All quantitative estimates are tied to these three assumptions, and we must recognize the choices and value judgements involved in the analysis when evaluating the ethical and legal implications of our findings.

Our analysis is further limited by the lack of data on how GHG emission compositions vary with income and wealth. This limits the accuracy of our results, given the role of non-CO_2 GHGs in recent warming. In addition, our drought indicator only considers precipitation, which may lead to underestimations in drought risks[24]. Finally, our analysis is based on modelled data, which may deviate from observations[44,45].

Accordingly, our analysis does not explicitly assign full responsibility for resulting climate impacts, nor does it determine fair emission levels for any income group. Such determinations require an integrated view of fairness, justice and socio-economic factors[46,47], with different reference points for societies at varying levels of development.

In conclusion, our findings demonstrate how individual emitter groups have contributed to increases in regional extremes globally. In times of growing economic and climate inequalities, advancing frameworks for attributing emissions to individual emitters can inform global climate action and enhance climate justice.

Online content

Any methods, additional references, Nature Portfolio reporting summaries, source data, extended data, supplementary information, acknowledgements, peer review information; details of author contributions and competing interests; and statements of data and code availability are available at https://doi.org/10.1038/s41558-025-02325-x.

References

1. Newman, R. & Noy, I. The global costs of extreme weather that are attributable to climate change. *Nat. Commun.* **14**, 6103 (2023).
2. Warner, K. & Weisberg, M. A funding mosaic for loss and damage. *Science* **379**, 219–219 (2023).
3. Chancel, L. Global carbon inequality over 1990–2019. *Nat. Sustain.* **5**, 931–938 (2022).
4. Wallemacq, P., Below, R. & McClean, D. *Economic Losses, Poverty and Disasters: 1998-2017* (United Nations Office for Disaster Risk Reduction, 2018); https://www.preventionweb.net/files/61119_credeconomiclosses.pdf
5. Diffenbaugh, N. S. & Burke, M. Global warming has increased global economic inequality. *Proc. Natl Acad. Sci. USA* **116**, 9808–9813 (2019).
6. Hallegatte, S. & Rozenberg, J. Climate change through a poverty lens. *Nat. Clim. Change* **7**, 250–256 (2017).
7. Dhakal, S. et al. in *Climate Change 2022: Mitigation of Climate Change* (eds Shukla, P. R. et al.) 215–294 (IPCC, Cambridge Univ. Press, 2023).
8. Mar, K. A., Unger, C., Walderdorff, L. & Butler, T. Beyond CO_2 equivalence: the impacts of methane on climate, ecosystems, and health. *Environ. Sci. Policy* **134**, 127–136 (2022).
9. Beusch, L., Gudmundsson, L. & Seneviratne, S. I. Emulating Earth system model temperatures with MESMER: from global mean temperature trajectories to grid-point-level realizations on land. *Earth Syst. Dynam.* **11**, 139–159 (2020).
10. Meinshausen, M., Raper, S. C. & Wigley, T. M. Emulating coupled atmosphere-ocean and carbon cycle models with a simpler model, MAGICC6 – part 1: model description and calibration. *Atmos. Chem. Phys.* **11**, 1417–1456 (2011).
11. Schöngart, S. Introducing the MESMER-M-TPv0.1.0 module: spatially explicit Earth system model emulation for monthly precipitation and temperature. *EGUsphere* **2024**, 8283–8320 (2024).
12. Otto, F. E. Attribution of extreme events to climate change. *Annu. Rev. Environ. Resour.* **48**, 813–828 (2023).
13. Stott, P. A., Stone, D. A. & Allen, M. R. Human contribution to the European heatwave of 2003. *Nature* **432**, 610–614 (2004).
14. Van Oldenborgh, G. J. et al. Pathways and pitfalls in extreme event attribution. *Climatic Change* **166**, 13 (2021).
15. Beusch, L. et al. Responsibility of major emitters for country-level warming and extreme hot years. *Commun. Earth Environ.* **3**, 7 (2022).
16. Callahan, C. W. & Mankin, J. S. National attribution of historical climate damages. *Climatic Change* **172**, 40 (2022).
17. Trudinger, C. & Enting, I. Comparison of formalisms for attributing responsibility for climate change: non-linearities in the brazilian proposal approach. *Climatic Change* **68**, 67–99 (2005).
18. Otto, F. E., Skeie, R. B., Fuglestvedt, J. S., Berntsen, T. & Allen, M. R. Assigning historic responsibility for extreme weather events. *Nat. Clim. Change* **7**, 757–759 (2017).
19. De Polt, K. et al. Quantifying impact-relevant heatwave durations. *Environ. Res. Lett.* **18**, 104005 (2023).
20. Seneviratne, S. et al. 2021: Weather and climate extreme events in a changing climate. in *Climate Change 2021: The Physical Science Basis. Contribution of Working Group I to the Sixth Assessment Report of the Intergovernmental Panel on Climate Change* (eds Masson-Delmotte, V. et al.), 1513–1766 (IPCC, Cambridge Univ. Press 2021).
21. Allen, M. R. et al. Indicate separate contributions of long-lived and short-lived greenhouse gases in emission targets. *npj Clim. Atmos. Sci.* **5**, 5 (2022).
22. Cook, B. I. et al. Twenty-first century drought projections in the CMIP6 forcing scenarios. *Earth Future* **8**, e2019EF001461 (2020).
23. Wu, Y. et al. Hydrological projections under CMIP5 and CMIP6: sources and magnitudes of uncertainty. *Bull. Am. Meteorol. Soc.* **105**, E59–E74 (2024).
24. Chen, D. et al. 2021: Framing, context, and methods. in *Climate Change 2021: The Physical Science Basis. Contribution of Working Group I to the Sixth Assessment Report of the Intergovernmental Panel on Climate Change* (eds Masson-Delmotte, V. et al.) 147–286 (IPCC, Cambridge Univ. Press, 2021).
25. Yao, Y., Ciais, P., Viovy, N., Joetzjer, E. & Chave, J. How drought events during the last century have impacted biomass carbon in amazonian rainforests. *Glob. Change Biol.* **29**, 747–762 (2023).

26. Kumar, N. et al. Joint behaviour of climate extremes across India: past and future. *J. Hydrol.* **597**, 126185 (2021).
27. McKenna, C. M., Maycock, A. C., Forster, P. M., Smith, C. J. & Tokarska, K. B. Stringent mitigation substantially reduces risk of unprecedented near-term warming rates. *Nat. Clim. Change* **11**, 126–131 (2021).
28. IPCC *Climate Change 2022: Impacts, Adaptation and Vulnerability* (eds Pörtner, H.-O. et al.) (Cambridge Univ. Press, 2023).
29. Zeppetello, L. R. V., Battisti, D. S. & Baker, M. B. The physics of heat waves: what causes extremely high summertime temperatures? *J. Clim.* **35**, 2231–2251 (2022).
30. Chancel, L., Bothe, P. & Voituriez, T. The potential of wealth taxation to address the triple climate inequality crisis. *Nat. Clim. Change* **14**, 5–7 (2024).
31. Zucman, G. *A Blueprint for a Coordinated Minimum Effective Taxation Standard for Utra-High-Net-Worth Individuals* (Tax Observatory, 2024); https://www.taxobservatory.eu/www-site/uploads/2024/06/report-g20-24_06_24.pdf
32. Pachauri, S. et al. Fairness considerations in global mitigation investments. *Science* **378**, 1057–1059 (2022).
33. Bhattacharya, A., Songwe, V., Soubeyran, E. & Stern, N. *Raising Ambition and Accelerating Delivery of Climate Finance* (Grantham Research Institute on Climate Change and the Environment, 2024); https://www.lse.ac.uk/granthaminstitute/wp-content/uploads/2024/11/Raising-ambition-and-accelerating-delivery-of-climate-finance_Third-IHLEG-report.pdf
34. Dibley, A. et al. Biases in 'sustainable finance' metrics could hinder lending to those that need it most. *Nature* **634**, 294–297 (2024).
35. Serdeczny, O. & Lissner, T. Research agenda for the loss and damage fund. *Nat. Clim. Change* **13**, 412–412 (2023).
36. Ogunbode, C. A. et al. Climate justice beliefs related to climate action and policy support around the world. *Nat. Clim. Change* **14**, 1144–1150 (2024).
37. Berger, J. & Liebe, U. Effective climate action must address both social inequality and inequality aversion. *npj Clim. Action* **4**, 1 (2025).
38. Jézéquel, A. et al. Broadening the scope of anthropogenic influence in extreme event attribution. *Environ. Res. Clim.* **3**, 042003 (2024).
39. Perkins-Kirkpatrick, S. E. et al. Frontiers in attributing climate extremes and associated impacts. *Front. Clim.* **6**, 1455023 (2024).
40. Noy, I. et al. Event attribution is ready to inform loss and damage negotiations. *Nat. Clim. Change* **13**, 1279–1281 (2023).
41. King, A. D., Grose, M. R., Kimutai, J., Pinto, I. & Harrington, L. J. Event attribution is not ready for a major role in loss and damage. *Nat. Clim. Change* **13**, 415–417 (2023).
42. Andrijevic, M. et al. Towards scenario representation of adaptive capacity for global climate change assessments. *Nat. Clim. Change* **13**, 778–787 (2023).
43. Smiley, K. T. et al. Social inequalities in climate change-attributed impacts of hurricane Harvey. *Nat. Commun.* **13**, 3418 (2022).
44. Jensen, L., Gerdener, H., Eicker, A., Kusche, J. & Fiedler, S. Observations indicate regionally misleading wetting and drying trends in CMIP6. *npj Clim. Atmos. Sci.* **7**, 249 (2024).
45. Kim, Y.-H., Min, S.-K., Zhang, X., Sillmann, J. & Sandstad, M. Evaluation of the CMIP6 multi-model ensemble for climate extreme indices. *Weather Clim. Extremes* **29**, 100269 (2020).
46. Zimm, C. et al. Justice considerations in climate research. *Nat. Clim. Change* **14**, 22–30 (2024).
47. Kikstra, J. S., Mastrucci, A., Min, J., Riahi, K. & Rao, N. D. Decent living gaps and energy needs around the world. *Environ. Res. Lett.* **16**, 095006 (2021).

Methods

We quantified intensity and frequency changes in extremely hot (dry) months attributable to specific emitter groups. The methodological framework relies on three steps (Fig. 1): first, we constructed counterfactual emissions pathways (that is, emissions pathways with and without the emissions of selected population groups); second, we translated emissions into gridded temperature, precipitation and potential drought data via a chain of computationally efficient emulators; and third, we built on the framework of extreme event attribution to quantify changes in the grid-cell-level distributions of the climatic variables.

We relied on the SPI-3 to identify meteorological droughts[20]. The SPI-3 is computed from precipitation data only, meaning that it does not account for changes in soil- and plant-based water demands. As climate-driven precipitation signals are dominated by natural variability and intermodel disagreement[24], climate change-induced trends in our drought indicator are probably a conservative estimate of actual changes[20]. Therefore, we also computed the SPEI-3[48]. The SPEI-3 takes changes in water demands via potential evapotranspiration (PET) into account. Ideally, PET is estimated from temperatures, radiation, wind speed and humidity via the Penman–Monteith equation[20,49]. Given that our emulation framework only depicts temperature and precipitation, we relied on the Thornthwaite method to compute PET from temperature data only[50]. However, PET estimates via the Thornthwaite method are prone to overestimations in terms of magnitude and temporal trends[51]. This left us with an indicator for meteorological droughts (SPI-3) that probably underestimates drought risks and an additional indicator for potential droughts (SPEI-3 via the Thornthwaite method) that probably provides an overestimation. We used the conservative estimates in the main part of our analysis and show potential drought risks in Supplementary Section 5.

Counterfactual emissions pathways

We assessed what our climate today would look like if the wealthiest 10%, 1% and 0.1% globally, as well as in the United States, EU27, India and China, had not contributed to global emissions between 1990 and 2019. We followed ref. 52 to construct a time series of historic baseline emissions from 1850–2019 resolved by gas. Next, we removed emitter-specific contributions from these baseline emissions (Fig. 1). To do so, we relied on a dataset of consumption-based CO_2e emissions categorized by country and income decile between 1990 and 2019[3]. The estimates relate to all emissions except those from agriculture, forestry and other land use. Our analysis required us to make assumptions about how to disaggregate the reported basket emissions into individual gases. We focused on decomposing emissions into CO_2, nitrogen oxide (N_2O) and CH_4. These three gases make up 98.7% of the total global GHG emissions (excluding agriculture, forestry and other land use)[53]. The composition of production-side GHG emissions varies strongly by country, ranging from primarily CO_2-based emissions (for example, Singapore) to almost equal shares of CO_2 and CH_4/N_2O (for example, Qatar) and, in low-income countries in particular, primarily CH_4/N_2O (for example, Chad)[54]. The carbon inequality dataset from ref. 3 employs input–output tables that redistribute production-side emissions to consumers across countries. About one-half of global CH_4 emissions are embodied in global trade, with household consumption dominating the final demand category[55]. Given these considerations, and a lack of alternative data, we chose to apply the same decomposition assumptions across countries and emitter groups. For our central estimate, we assumed that emissions for each GHG scale proportionally with the globally aggregated emissions. We tested the sensitivity to this assumption by providing two extreme cases in which the wealthy emitters (1) solely emit carbon (CO_2case) or (2) solely emit CH_4 and N_2O (non-CO_2case). Note that in the non-CO_2 case, the emissions associated with the global top 10% are larger than the total global CH_4 and N_2O emissions combined, and we removed the excessive emissions from the CO_2 time series. We converted between individual GHGs and CO_2e using the Global Warming Potential 100.

Emulator-based modelling approach

We transformed counterfactual emissions into grid-cell-level distributions of temperature and precipitation using emulators and subsequently computed drought measures from the emulated data. The emulation consisted of two steps: first, converting emissions into GMT; and second, translating GMT into grid-cell-level monthly mean temperature and precipitation distributions (Fig. 1). The first translation step was carried out with MAGICC[10,56]. MAGICC is a simple, computationally efficient climate model for global climate indicators. Our temperature outcomes were calculated with MAGICC v7.5 in a probabilistic setting that reflects the assessed uncertainty ranges from the IPCC's Sixth Assessment Report[24]. We generated 600 GMT trajectories for each scenario. The second translation step was carried out using MESMER-M-TP[11]. MESMER-M-TP combines parametric approaches and stochastic sampling to approximate the behaviour of individual climate models. For any climate model, the emulator can be calibrated with a small set of actual climate model data and then used to generate gridded temperature and precipitation data that statistically resemble the climate model data. Here we calibrated MESMER-M-TP with 24 different models from the Phase Six of the Coupled Model Intercomparison Project (Supplementary Table 4). Subsequently, we converted each GMT trajectory into a single gridded time series of temperature and precipitation. We computed the SPI-3/SPEI-3 indicator following ref. 48 and used the gamma distribution for normalization. This provided us with a dataset containing 4 variables × 600 realizations × 2,652 grid points × 170 years × 12 months for each scenario.

Attribution framework

Traditional attribution studies typically aim to understand how climate change altered the statistics of a specified observed extreme. Our study deviates from this approach. We were interested in understanding the extent to which changes in a broad class of historic extremes can be related to emissions from specific emitter groups. We therefore used the framework for event attribution as a guideline[14] but modified it according to our research questions. Most importantly, our analysis fully relied on modelled data, meaning that we were not taking observational data into account. Hence, the event attribution framework was reduced to three essential steps: first, we defined extreme events; second, we performed an analysis using emulated (climate model) data; and third, we synthesized the hazards into an attribution statement.

Extreme event definition

We defined extreme events relative to the reference period 1850–1900 and focused on 1-in-100-year (main text) and 1-in-50/1-in-10,000-year (Supplementary Information) events.

Climate model analysis and hazard synthesis

In a first step, we tested whether changes in the grid-cell-level distribution of a climatic variable under a given counterfactual scenario were significantly different from its present-day distribution. To this end, we computed the differences between the present-day and counterfactual present-day distributions and employed a Student's *t*-test[57] to verify that the distribution was significantly different from zero. If this was the case, we proceeded with the actual attribution. We used the modelled distribution of climatic variables over the reference period to derive grid-cell-specific intensity thresholds for our defined events. To assess frequency changes, we counted how many times the reference intensity threshold was exceeded in a present-day (2020) climate and in a counterfactual 2020 climate, and attributed the difference to a specific emitter group. Similarly, we quantify intensity changes by assessing how hot (dry) a specific extreme would be in a present-day

climate as compared to a counterfactual climate, and attribute the difference in values.

Reporting summary

Further information on research design is available in the Nature Portfolio Reporting Summary linked to this article.

Data availability

The data generated for this study are available via Zenodo at https://doi.org/10.5281/zenodo.14860538 (ref. 58). The results can be reproduced using public data records. The starting point of our analysis was time series of per capita CO_2e emissions from ref. 3. We also used historic emissions data available in ref. 52. We used MAGICC v7.5 (refs. 10,56) to translate our input data into GMT levels and MESMER-M-TPv0.1.0 (refs. 11,59) to generate a large ensemble of temperature and precipitation data.

Code availability

Our code is publicly available via GitHub at https://github.com/sarasita/attribution.git. The exact version used to produce this study is available via Zenodo at https://doi.org/10.5281/zenodo.15011461 (ref. 60). Note, parts of our code rely on processing data according to ref. 60.

References

48. Tirivarombo, S., Osupile, D. & Eliasson, P. Drought monitoring and analysis: standardised precipitation evapotranspiration index (SPEI) and standardised precipitation index (SPI). *Phys. Chem. Earth, Parts A/B/C.* **106**, 1–10 (2018).
49. Vicente-Serrano, S. M., Van der Schrier, G., Beguería, S., Azorin-Molina, C. & Lopez-Moreno, J.-I. Contribution of precipitation and reference evapotranspiration to drought indices under different climates. *J. Hydrol.* **526**, 42–54 (2015).
50. Santos, C. N. et al. Monthly potential evapotranspiration estimated using the Thornthwaite method with gridded climate datasets in southeastern brazil. *Theor. Appl. Climatol.* **155**, 3739–3756 (2024).
51. Sheffield, J., Wood, E. F. & Roderick, M. L. Little change in global drought over the past 60 years. *Nature* **491**, 435–438 (2012).
52. Nicholls, Z. R. J. et al. Reduced complexity model intercomparison project phase 1: introduction and evaluation of global-mean temperature response. *Geosci. Model Dev.* **13**, 5175–5190 (2020).
53. IPCC: Summary for policymakers. In *Climate Change 2022: Mitigation of Climate Change* (eds Shukla, P. R. et al.) (Cambridge Univ. Press, 2023).
54. Gütschow, J. et al. The PRIMAP-hist national historical emissions time series. *Earth Syst. Sci. Data* **8**, 571–603 (2016).
55. Zhang, B. et al. Consumption-based accounting of global anthropogenic CH_4 emissions. *Earth Future* **6**, 1349–1363 (2018).
56. Meinshausen, M. et al. Greenhouse-gas emission targets for limiting global warming to 2 °C. *Nature* **458**, 1158–1162 (2009).
57. Büning, H. & Trenkler, G. *Nichtparametrische Statistische Methoden* (Walter de Gruyter, 2013).
58. Schoengart, S. Data accompanying publication "High-Income Groups Disproportionately Contribute to Climate Extremes Worldwide.". *Zenodo* https://doi.org/10.5281/zenodo.14860538 (2025).
59. Schöngart, S. sarasita/mesmer-m-tp: MESMER-M-TP v0.1.0 - GMD Submission. *Zenodo* https://doi.org/10.5281/zenodo.11086167 (2024).
60. Schöngart, S. sarasita/attribution: code version accompanying publication "High-Income Groups Disproportionately Contribute to Climate Extremes Worldwide.". *Zenodo* https://doi.org/10.5281/zenodo.15011461 (2025).

Acknowledgements

S.S. acknowledges support from the German Federal Environmental Foundation (DBU). S.S. and C.F.S. acknowledge funds from the European Union's Horizon 2020 Research and Innovation Programme under grant number 101003687 (PROVIDE). C.F.S. acknowledges funds from the European Union's Horizon Europe Programme under grant number 101081369 (SPARCCLE). Z.N. acknowledges support from the European Union's Horizon 2020 Research and Innovation Funding Programme (grant number 101003536, Earth System Models for the Future, ESM2025). R.H. acknowledges funding from the European Union's Horizon Europe Programme under grant agreement number 101094551 (SPES) and grant agreement number 101162653 (2C-RISK) supported by the European Research Council. S.P. acknowledges funding from the European Union's Horizon Europe Research and Innovation Programme under grant number 101056873 (ELEVATE). We also gratefully acknowledge funding from IIASA and the National Member Organizations that support the institute. Views and opinions expressed are those of the author(s) only and do not necessarily reflect those of the European Union or the European Research Council Executive Agency. Neither the European Union nor the granting authority can be held responsible for them.

Author contributions

S.S., Z.N., R.H., S.P. and C.-F.S. conceived the study. S.S. performed the data analysis with contributions from Z.N. S.S. wrote the manuscript with contributions from Z.N., R.H., S.P. and C.-F.S. S.S., Z.N., R.H., S.P. and C.-F.S. have read and agreed to the published version of the manuscript.

Funding

Open access funding provided by Swiss Federal Institute of Technology Zurich

Competing interests

The authors declare no competing interests.

Additional information

Supplementary information The online version contains supplementary material available at https://doi.org/10.1038/s41558-025-02325-x.

Correspondence and requests for materials should be addressed to Sarah Schöngart.

Peer review information *Nature Climate Change* thanks Christopher Callahan and the other, anonymous, reviewer(s) for their contribution to the peer review of this work.

nature portfolio

Corresponding author(s): Sarah Schöngart

Last updated by author(s): 13/03/2025

Reporting Summary

Nature Portfolio wishes to improve the reproducibility of the work that we publish. This form provides structure for consistency and transparency in reporting. For further information on Nature Portfolio policies, see our Editorial Policies and the Editorial Policy Checklist.

Statistics

For all statistical analyses, confirm that the following items are present in the figure legend, table legend, main text, or Methods section.

n/a	Confirmed	
☐	☒	The exact sample size (*n*) for each experimental group/condition, given as a discrete number and unit of measurement
☒	☐	A statement on whether measurements were taken from distinct samples or whether the same sample was measured repeatedly
☒	☐	The statistical test(s) used AND whether they are one- or two-sided *Only common tests should be described solely by name; describe more complex techniques in the Methods section.*
☒	☐	A description of all covariates tested
☒	☐	A description of any assumptions or corrections, such as tests of normality and adjustment for multiple comparisons
☐	☒	A full description of the statistical parameters including central tendency (e.g. means) or other basic estimates (e.g. regression coefficient) AND variation (e.g. standard deviation) or associated estimates of uncertainty (e.g. confidence intervals)
☒	☐	For null hypothesis testing, the test statistic (e.g. *F*, *t*, *r*) with confidence intervals, effect sizes, degrees of freedom and *P* value noted *Give P values as exact values whenever suitable.*
☒	☐	For Bayesian analysis, information on the choice of priors and Markov chain Monte Carlo settings
☒	☐	For hierarchical and complex designs, identification of the appropriate level for tests and full reporting of outcomes
☒	☐	Estimates of effect sizes (e.g. Cohen's *d*, Pearson's *r*), indicating how they were calculated

Our web collection on statistics for biologists contains articles on many of the points above.

Software and code

Policy information about availability of computer code

Data collection	The data generated for this study is available at https://zenodo.org/records/14860538. The results can be reproduced using public data records. CO2-e per capita emissions are available from https://lucaschancel.com/global-carbon-inequality-1990-2019/. We take historic emissions from https://gmd.copernicus.org/articles/13/5175/2020/ and references therein.
Data analysis	We rely on MAGICC v7.5 (https://magicc.org/download/magicc7) to translate our input data into GMT levels. We then rely on MESMER-M-TPv0.1.0 (https://github.com/sarasita/mesmer-m-tp.git) to generate a large-ensemble of temperature and precipitation data. Our code is available at https://github.com/sarasita/attribution.git and archived at https://zenodo.org/records/15011461.

For manuscripts utilizing custom algorithms or software that are central to the research but not yet described in published literature, software must be made available to editors and reviewers. We strongly encourage code deposition in a community repository (e.g. GitHub). See the Nature Portfolio guidelines for submitting code & software for further information.

Data

Policy information about availability of data

All manuscripts must include a data availability statement. This statement should provide the following information, where applicable:

- Accession codes, unique identifiers, or web links for publicly available datasets
- A description of any restrictions on data availability
- For clinical datasets or third party data, please ensure that the statement adheres to our policy

The data generated for this study is available at ref. [34] (https://doi.org/10.5281/zenodo.14039672). The results can be reproduced using public data records as outlined in the paper.

Human research participants

Policy information about studies involving human research participants and Sex and Gender in Research.

Reporting on sex and gender	n/a
Population characteristics	n/a
Recruitment	n/a
Ethics oversight	n/a

Note that full information on the approval of the study protocol must also be provided in the manuscript.

Field-specific reporting

Please select the one below that is the best fit for your research. If you are not sure, read the appropriate sections before making your selection.

☐ Life sciences ☐ Behavioural & social sciences ☒ Ecological, evolutionary & environmental sciences

For a reference copy of the document with all sections, see nature.com/documents/nr-reporting-summary-flat.pdf

Ecological, evolutionary & environmental sciences study design

All studies must disclose on these points even when the disclosure is negative.

Study description	We generate counterfactual emission pathways by subtracting the 1990-2019 emissions of specific emitter groups, namely the wealthiest 10%/1%/0.1% globally, as well as in the US, the EU27, India, and China. We then convert these counterfactual pathways into GMT levels and gridded climatic variables, allowing us to compare the 2020 climate against the hypothetical 2020 climate state that we would observe, if these groups had not emitted. Specifically, we attribute GMT levels and changes in the probability and intensity of monthly temperature and meteorological drought extremes to the specified emitter groups.
Research sample	We rely on an emulator based modeling approach that approximates the behavior of 24 different Earth System Models. For each (counterfactual) emission pathway we generate an ensemble of 600 gridded temperature and potential drought realizations at monthly resolution.
Sampling strategy	Sample size was chosen in consistency with IPCC's AR6 uncertainty ranges from MAGICC v7.5.
Data collection	Sa.S. collected the data through public repositories.
Timing and spatial scale	Temperature, precipitation and drought data is at monthly resolution and covers a 2.5°x2.5° latitude-longitude grid.
Data exclusions	No data was excluded from the analysis.
Reproducibility	Results are reproducible using public data repositories and the code we provide (https://github.com/sarasita/attribution.git). We stored random seeds whenever our approach relied on stochastic processes. These can be made available upon request.
Randomization	n/a
Blinding	n/a

Did the study involve field work? ☐ Yes ☒ No

Reporting for specific materials, systems and methods

We require information from authors about some types of materials, experimental systems and methods used in many studies. Here, indicate whether each material, system or method listed is relevant to your study. If you are not sure if a list item applies to your research, read the appropriate section before selecting a response.

Materials & experimental systems

n/a	Involved in the study
☒	☐ Antibodies
☒	☐ Eukaryotic cell lines
☒	☐ Palaeontology and archaeology
☒	☐ Animals and other organisms
☒	☐ Clinical data
☒	☐ Dual use research of concern

Methods

n/a	Involved in the study
☒	☐ ChIP-seq
☒	☐ Flow cytometry
☒	☐ MRI-based neuroimaging